Ab Initio MO Study of the Cationic States of 1,3,5-Triazine and Hexahydro-1,3,5-triazine

Takeshi Saito, Akihiro Ito, and Kazuyoshi Tanaka*

Department of Molecular Engineering, Graduate School of Engineering, Kyoto University, Sakyo-ku, Kyoto 606-8501, Japan

Received: March 24, 1998; In Final Form: July 10, 1998

Electronic structures of cationic states (2^+ and 3^+) of 1,3,5-triazine (TA) and its derivative hexahydro-1,3,5-triazine (HTA) are discussed with the ab initio molecular-orbital method including the electron correlation by the Møller−Plesset (MP) perturbation treatment. It has been found that σ-radical spins give rise to low- and high-spin states in both TA and HTA. The present calculation at the MP3 level predicts that the spin multiplicity of the ground state of dicationic TA is a high-spin state triplet while that of tricationic TA is a doublet. On the other hand, low- and high-spin states are almost degenerate in both the dicationic and the tricationic states of HTA. This result will hopefully lead to the discovery of a high-spin state occurring from σ-radical spins in molecules containing heteroatoms as the spin accommodators.

1. Introduction

Ferromagnetism was not expected to exist in compounds consisting only of light elements such as carbon, hydrogen, oxygen, and nitrogen.[1] However, since the first organic ferromagnet was reported by Kinoshita et al. in 1991,[2] much attention has been paid to the chemistry of high-spin molecules and to the search for the possibility of the organic ferromagnetic materials. Extensive work[3−7] has focused on the design of high-spin molecules as the first step to obtain organic ferromagnets.

In general, high-spin molecules have *n*-fold degenerate or quasi-degenerate singly occupied molecular orbitals (SOMO's), and therefore, their ground states will be of a high-spin state in which the total spin quantum number (S) is equal to $n/2$ by application of Hund's rule. In addition to this basic rule, Borden and Davidson have proposed that it is useful for understanding the spin configuration of the ground state of the diradical to classify it into two types according to whether its nonbonding MO's (NBMO's) are confined into disjoint or nondisjoint sets of atoms in terms of the electron correlation.[8] Most of the high-spin molecules discovered belong to non-Kekulé π-conjugated hydrocarbons (occasionally containing heteroatoms),[9,10] and these molecules have been well-investigated theoretically.[11] For example, the electronic structure of the trication triradical of 1,3,5-tris(diphenylamino)benzene (TDAB) and its derivatives have been studied experimentally[10] and theoretically,[11] the ground state of $TDAB^{3+}$ being confirmed to be a quartet state.

Meanwhile, several ferromagnetic organic amorphous materials prepared by pyrolysis[12−14] or chemical vapor deposition (CVD)[15−18] have been reported. Some of these materials have been mentioned to have σ-spin radicals for their ferromagnetic origin and not to belong to the class of the above-mentioned non-Kekulé π-conjugated compounds.[17] However, these seem to suffer from poor reproducibility of the ferromagnetic fraction and, especially, incomplete characterization. Recently, a prototypical system of nonconjugated hydrocarbons has been preliminary studied by the semiempirical MO method dealing with the spin interaction,[19] although the geometry optimizations were carried out with the constraint to high symmetry and the effect of Jahn−Teller distortion to the low-spin state was not taken into account. Nonetheless, such a system is intriguing in that it could form a new class of organic ferromagnetic materials and is worth investigating.

From this point of view, a study on the electronic structures of cationic radicals of heterocyclic compounds without π-conjugation would be also of interest as a model in order to investigate the spin interaction in a nonconjugated system. In the present article, we report the ab initio MO investigation of cationic states of 1,3,5-triazine (TA) and hexahydro-1,3,5-triazine (HTA), shown in Figure 1, based on the Møller−Plesset (MP) perturbation theory, in order to clarify the electronic structures of the cationic states and, in particular, to predict the spin multiplicity of each ground state. Although there have been several theoretical studies on TA[20,21] and HTA,[22] to our knowledge, the investigation on di- and tricationic species has not been carried out. In these molecules, nitrogen atoms are expected to stably accommodate the radical spins; furthermore, comparison of the nature of the spins in TA and HTA would be also of interest. The role of the methylene groups in HTA as the ferromagnetic coupling units is also discussed.

2. Method of Calculation

First, let us express neutral, dicationic closed-shell singlet, dicationic open-shell singlet, dicationic triplet, tricationic doublet, and tricationic quartet states of HTA in terms of HTA^0, $^1HTA^{2+}$, $^1HTA^{2+}$ (OSS), $^3HTA^{2+}$, $^2HTA^{3+}$, and $^4HTA^{3+}$, respectively, for simplicity. Similar notations are used for TA as well. For the calculation of these spin-state problems, the CAS (complete active space) SCF method is probably the most suitable procedure. In the present calculations, however, this method failed to give the geometry optimized results due to the convergence problem. Hence, the geometry optimizations were carried out for these states at the unrestricted Hartree−Fock (UHF) level using the 6-31G* basis set. It is well-known that difficulty occurs when using the UHF method for Jahn−Teller distortion in the open-shell compounds with degenerate MO's, such as, e.g., cyclopropenyl radical,[23] because of spin contamination. On the other hand, the spin contaminations for

S1089-5639(98)01601-6 CCC: $15.00
Published on Web 09/22/1998

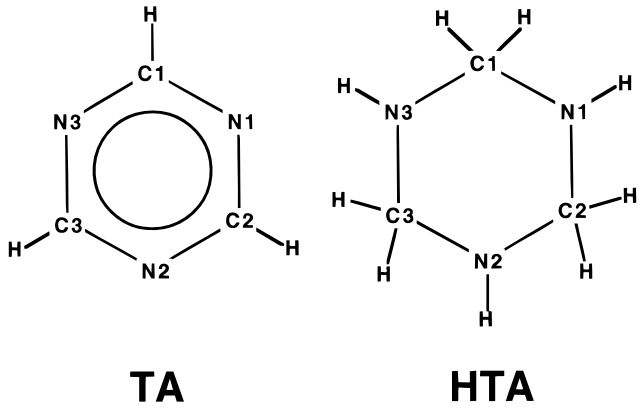

Figure 1. Triazine (TA) and hexahydro-1,3,5-triazine (HTA).

the present systems were estimated to be quite low, as described in a later section. Furthermore, according to ref 24, the UHF method affords better geometries for high-spin molecules than the ROHF method does. Therefore, the UHF method would be pertinent to the present systems.

In this study, to complement our results, the electron correlation was included by means of the MP perturbation scheme (MP2 and MP3/6-31G*) in addition to the UHF/6-31G* calculations, since the MP perturbation method has been successfully applied to the Jahn−Teller distortions of benzene cations,[25] ammonia cation,[26] methoxy radical,[27] and substituted cyclopentane cations.[28] All of the calculations in the present study were carried out with the Gaussian 94 program.[29]

3. Geometry Optimization of TA and HTA

3.1. TA. Typical structural parameters in the optimized structures of the neutral and several cationic TA molecules are listed in Table 1. First, to include a static Jahn−Teller effect on each of the cationic states, we carried out those optimizations under the constraint of C_{2v} symmetry, except for TA^0 and $^1TA^{2+}$ (OSS). The optimized structure of TA^0 is planar and 3-fold symmetric, i.e., of full D_{3h} symmetry (Table 1). For $^1TA^{2+}$ (OSS), we adopt the geometry optimization under the constraint of the C_s symmetry because we consider that the molecular structure of $^1TA^{2+}$ (OSS) cannot retain a higher symmetry like $^3TA^{2+}$ by application of the Hund's rule. Among those structures optimized under the constraint of C_{2v} symmetry, however, $^3TA^{2+}$ and $^4TA^{3+}$ are very likely to have D_{3h} symmetry. Both in $^1TA^{2+}$ and $^2TA^{3+}$, we obtained two kinds of optimized structures, labeled I and II. The raison d'être of these two kinds of structures and the lowest lying states of $^1TA^{2+}$ and $^2TA^{3+}$ will be discussed in detail in the following section.

Surprisingly, in $^1TA^{2+}$ (I), the atomic distance between N1 and N3 becomes considerably shorter, only 1.512 Å, and there seems to be a bonding nature between these two atoms. According to the full Mulliken population analysis, pσ−pσ bond population is equal to 0.203 whereas the total atomic bond population is 0.093. Therefore, the bonding nature between N1 and N3 is almost of a pure σ-type.

3.2. HTA. Selected structural parameters in the optimized structures of the neutral and several cationic HTA molecules are listed in Table 2 with their characterizations. By the same reason as that in TA, the geometry optimizations were carried out under the constraint of C_s symmetry for $^1HTA^{2+}$ (OSS), $^3HTA^{2+}$, and $^2HTA^{3+}$ and of D_{3h} symmetry for $^1HTA^{2+}$ and $^4HTA^{3+}$. It has been found that the triazine rings of $^1HTA^{2+}$ and $^4HTA^{3+}$ are planar, whereas HTA^0, $^3HTA^{2+}$, and $^2HTA^{3+}$ are nonplanar. Specifically, the ring of HTA^0 is of a chair type and $^3HTA^{2+}$ is of a boat type. The ring of $^2HTA^{3+}$ is almost planar but slightly warped into a boat shape. The optimized bond lengths in the high-spin states of HTA^{2+} and HTA^{3+} are longer than those in the low-spin states. This is more remarkable in $^3HTA^{2+}$; each bond length and the N−N distances are considerably different from those of $^1HTA^{2+}$.

4. Spin Contamination and Quality of Calculations

In general, a UHF function is contaminated by higher multiplicity components as a result of different spatial orbitals for different spins. When these are quite large, it is impossible to compare the energies of those open-shell states directly. From this point of view, attention must be paid to the quality of the present UHF calculations. In Table 3 are listed the calculated energies and the expectation values of the total spin operator $\langle S^2\rangle$ at the UHF level. Note that two or three low-lying electronic structures are found to exist in $^1TA^{2+}$, $^2TA^{3+}$, and $^1HTA^{2+}$.

Let us consider here the spin contamination of cationic TA, except the open-shell singlet state $^1TA^{2+}$ (OSS) which we will discuss in detail with $^1HTA^{2+}$ (OSS) at the end of this section. The calculated $\langle S^2\rangle$ values for $^2TA^{3+}$ (I), $^2TA^{3+}$ (II), $^3TA^{2+}$, and $^4TA^{3+}$ are 0.841, 1.012, 2.185, and 3.920, respectively, while the $\langle S^2\rangle$ values for pure doublets, triplets, and quartets are 0.75, 2, and 3.75, respectively (Table 3). Here, assuming that only $S' = S + 1$ is the spin contamination, the spin contamination ratio α[30] defined by

$$\alpha = \frac{{c_{S+1}}^2}{{c_S}^2 + {c_{S+1}}^2} \times 100 \qquad (1)$$

where

$$\langle S^2\rangle_{\mathrm{UHF}} = {c_S}^2\langle S^2\rangle + {c_{S+1}}^2\langle (S+1)^2\rangle \qquad (2)$$

is estimated to be ca. 3.0%, 8.7%, 4.6%, and 3.4%, respectively, for $^2TA^{3+}$ (I), $^2TA^{3+}$ (II), $^3TA^{2+}$, and $^4TA^{3+}$. These weights are rather small, so that the UHF calculation energy of each state is regarded to be approximately correct. In this sense, the energies of $^2TA^{3+}$ (I) and $^2TA^{3+}$ (II) can be compared, shown in Table 3, giving the lowest lying state as $^2TA^{3+}$ (II).

On the other hand, the $\langle S^2\rangle$ values for $^2HTA^{3+}$, $^3HTA^{2+}$, and $^4HTA^{3+}$ were 0.893, 2.001, and 3.751, respectively, so the spin contamination is nearly negligible for triplets and quartets. Assuming that the contamination in this doublet state also comes only from the quartet state ($S + 1$) as in TA, the quartet contamination ratio in $^2HTA^{3+}$ is estimated to be ca. 4.8%. This is quite small and therefore, the calculated UHF energy of $^2HTA^{3+}$ is considered to be approximately correct.

The spin contaminations of $^1TA^{2+}$ (OSS) and $^1HTA^{2+}$ (OSS) are rather complex: The $\langle S^2\rangle$ values for $^1TA^{2+}$ (OSS) and $^1HTA^{2+}$ (OSS) are 0.835 and 0.332, respectively. Hence, the values of the triplet contamination ratio in $^1TA^{2+}$ (OSS) and $^1HTA^{2+}$ (OSS) are estimated to be ca. 41.8% and 16.6%, respectively. These values are quite large, and the calculated OSS states must involve the corresponding triplet (and/or higher-spin) state. Therefore, the calculated energies of $^1TA^{2+}$ (OSS) and $^1HTA^{2+}$ (OSS) should differ from those for the pure OSS states. Note, however, these OSS species are calculated to be more unstable than the corresponding triplet states (Table 3).

5. Electronic Structures

5.1. Neutral State. First, let us consider the electronic structure of the neutral states, TA^0 and HTA^0, as the reference

TABLE 1: Optimized Structures and Their Bond Lengths[a] of TA Species at the UHF/6-31G* Level

	TA^0	$^1TA^{2+}$ (I)[b]	$^1TA^{2+}$ (II)[c]	$^1TA^{2+}$ (OSS)	$^3TA^{2+}$	$^2TA^{3+}$ (I)[d]	$^2TA^{3+}$ (II)[e]	$^4TA^{3+}$
shape of triazine ring	planar	planar	planar	pseudoplanar	planar	planar	planar	planar
point group	D_{3h}	C_{2v}	C_{2v}	C_s	D_{3h}	C_{2v}	C_{2v}	D_{3h}
state	$^1A_{1'}$	$^1A_1$	$^1A_1$	$^1A''$	$^3A_{2'}$	$^2A_1$	$^2B_2$	$^4A_{2'}$
C1−N1	1.318	1.290	1.319	1.328	1.327	1.317	1.330	1.339
N1−C2	1.318	1.348	1.320	1.309	1.327	1.338	1.333	1.339
C2−N2	1.318	1.314	1.305	1.329	1.327	1.350	1.330	1.339
N2−C3	1.318	1.314	1.305	1.329	1.327	1.350	1.330	1.339
C3−N3	1.318	1.348	1.320	1.309	1.327	1.338	1.333	1.339
N3−C1	1.318	1.290	1.319	1.328	1.327	1.317	1.330	1.339
N1−N2	2.345	2.195	2.073	2.208	2.197	2.071	2.149	2.182
N2−N3	2.345	2.195	2.073	2.208	2.197	2.071	2.149	2.182
N3−N1	2.345	1.512	2.326	2.217	2.197	1.449	2.192	2.182

[a] The numbering of the carbon and nitrogen atoms correspond to those of Figure 1. [b] The more stable form where the HOMO belongs to $e'(a_1)$ of TA^0 (see text). [c] The HOMO belongs to $e'(b_2)$ of TA^0 (see text). [d] The SOMO belongs to $e'(a_1)$ of TA^0 (see text). [e] The more stable form where the SOMO belongs to $e'(b_2)$ of TA^0 (see text).

TABLE 2: Optimized Structures and Their Bond Lengths[a] of HTA Species at the UHF/6-31G* Level

	HTA^0	$^1HTA^{2+}$	$^1HTA^{2+}$ (OSS)	$^3HTA^{2+}$	$^2HTA^{3+}$	$^4HTA^{3+}$
shape of triazine ring	nonplanar (chair-type)	planar	nonplanar (boat-type)	nonplanar (boat-type)	pseudoplanar	planar
point group	C_s	D_{3h}	C_s	C_s	C_s	D_{3h}
state	$^1A'$	$^1A_{1'}$	$^1A''$	$^3A''$	$^2A''$	$^4A_{1''}$
C1−N1	1.449	1.389	1.443	1.460	1.465	1.470
N1−C2	1.454	1.389	1.439	1.500	1.462	1.470
C2−N2	1.444	1.389	1.476	1.414	1.461	1.470
N2−C3	1.444	1.389	1.476	1.414	1.461	1.470
C3−N3	1.454	1.389	1.439	1.500	1.462	1.470
N3−C1	1.449	1.389	1.443	1.460	1.465	1.470
N1−N2	2.387	2.355	2.372	2.311	2.418	2.423
N2−N3	2.387	2.355	2.372	2.311	2.418	2.423
N3−N1	2.350	2.355	2.123	2.380	2.410	2.423

[a] The numbering of the carbon and nitrogen atoms correspond to those of Figure 1.

TABLE 3: Calculated Energies and Expectation Values of the Total Spin Operator $\langle S^2 \rangle$ at the UHF Level

	energy (UHF)/hartree	E_{rel}[a]/kcal·mol^{-1}	$\langle S^2 \rangle$[b]
$^1TA^{2+}$ (I)	−277.7246	+47.88	0 (0)
$^1TA^{2+}$ (II)	−277.6815	+74.92	0 (0)
$^1TA^{2+}$ (OSS)	−277.7751	+16.19	0.835 (0)
$^3TA^{2+}$	−277.8009	0	2.185 (2)
$^2TA^{3+}$ (I)	−276.9345	+40.85	0.841 (0.75)
$^2TA^{3+}$ (II)	−277.0063	−4.20	1.012 (0.75)
$^4TA^{3+}$	−276.9996	0	3.920 (3.75)
$^1HTA^{2+}$	−281.3376	+74.61	0 (0)
$^1HTA^{2+}$ (OSS)	−281.4412	+ 9.60	0.332 (0)
$^3HTA^{2+}$	−281.4565	0	2.001 (2)
$^2HTA^{3+}$	−280.8023	−0.25	0.893 (0.75)
$^4HTA^{3+}$	−280.8019	0	3.751 (3.75)

[a] Energy relative to the corresponding high-spin state, where the positive value signifies the instability. [b] In parentheses is shown the value for the pure multiplet state.

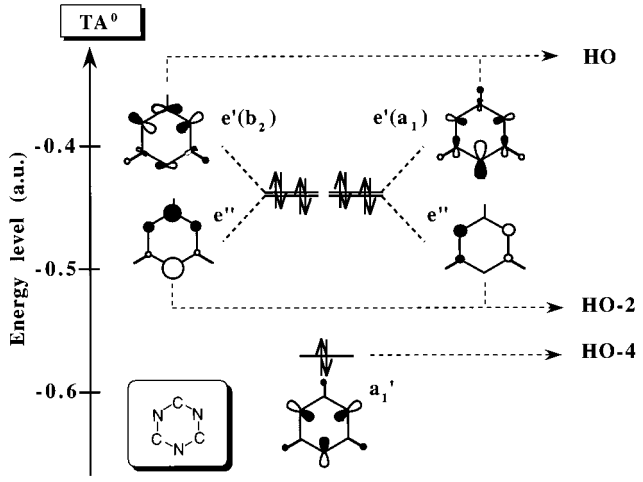

Figure 2. Energy levels and patterns of the frontier MO's of TA^0.

for further discussion. The energy levels of the MO's near the highest occupied (HO) MO and their orbital patterns are shown in Figures 2 and 3, respectively.

In TA^0 it is seen that the HO → (HO-2) MO's are almost 4-fold degenerate. Although for D_{3h} symmetry the degenerate HOMO's should be labeled as e′, the labeling for C_{2v} symmetry is also shown in Figure 2 for the purpose of discrimination between these MO's. Note that the HO and (HO-4) MO's, labeled e′ and a_1', respectively, have σ character, in contrast with those of benzene having π character. The present HO and (HO-4) MO's can be regarded as nonbonding (NB) MO's, mainly originating from the nitrogen lone pairs. On the other hand, it is found that the HO → (HO-2) MO's of HTA^0 in Figure3 are almost 3-fold degenerate, and these can also be regarded as NBMO's, again composed of the nitrogen lone pairs.

5.2. Cationic States. First, let us consider the electronic structures of cationic TA species compared with that of TA^0. The frontier MO patterns of all the cationic TA's are quite similar to the corresponding ones of TA^0, and therefore, the labels for the MO in Figure 2 are employed for the following discussion.

Closed-shell $^1TA^{2+}$ species would be expected to have $e'(a_1)$ or $e'(b_2)$ as the HOMO, and hence, two kinds of electronic structures are expected in $^1TA^{2+}$. In fact, two optimized structures ($^1TA^{2+}$ I and II) were obtained (see Table 1). $^3TA^{2+}$

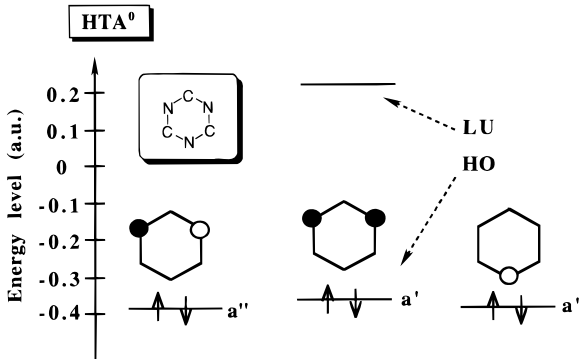

Figure 3. Energy levels and patterns of the frontier MO's of HTA^0.

(or $^1TA^{2+}$ (OSS)) would be expected to have both e′(a_1) and e′(b_2) as the SOMO's, electron spins in which triplets (or open-shell singlets) would form. As shown in Table 1, the electronic state of $^1TA^{2+}$ (I) is $^1A_1$. The HOMO pattern of $^1TA^{2+}$ (I) is represented by e′(a_1), whose pattern clearly shows the above-mentioned σ-type bonding nature between N1 and N3 being directly reflected in the considerably shorter atomic distance. A quite similar σ-type bonding nature has been observed in 1,3-didehydrobenzene (*m*-benzyne) both experimentally[31] and theoretically.[32] On the other hand, the electronic state of $^3TA^{2+}$ is $^3A_2'$, as listed in Table 1, and its α-SOMO patterns are similar to those of e′(a_1) and e′(b_2). Since these SOMO's are considerably spin-correlated with the σ-type a_1' orbital rather than the π-type e″ ones due to the strong exchange interaction, the highest occupied β-SOMO is of a_1' symmetry in $^3TA^{2+}$. Moreover, we can expect that the α-SOMO's of $^4TA^{3+}$ consist of e′(a_1), e′(b_2), and a_1'.

Furthermore, $^2TA^{3+}$ would have a SOMO whose pattern is like that of e′(a_1) or e′(b_2) of TA^0 in Figure 2, and hence, as listed in Table 1, there can be two kinds of electronic structures, $^2TA^{3+}$ (I) and (II) similar to $^1TA^{2+}$. The electronic state of $^2TA^{3+}$ (II) is $^2B_2$, and its SOMO pattern is similar to that of e′(b_2) (σ-type) of TA^0. On the other hand, the electronic state of $^4TA^{3+}$ is $^4A_2'$, and the patterns of the three SOMO's are similar to those of e′(a_1), e′(b_2), and a_1', as expected from the electronic state of $^3TA^{2+}$.

In cationic HTAs other than $^3HTA^{2+}$, their MO patterns near the HO level, shown in Figure 4, are of pseudo-π-type and rather different from those of HTA^0. With respect to $^3HTA^{2+}$, it is found that the SOMO's are almost 2-fold degenerate NBMO's (see Figure 4a). The energy levels of the π-type MO's and their orbital patterns of $^1HTA^{2+}$ are extracted in Figure 5. It should be mentioned that this clearly indicates that there are 10 π-electrons, conforming to the Hückel's rule with the aid of the hyperconjugation on the methylene groups. Because of this pseudoaromaticity, the optimized structure of $^1HTA^{2+}$ would favor a planar triazine ring and shorter bond lengths (see Table 2).

5.3. Effects of Electron Repulsion in Dicationic States of TA and HTA. As mentioned above, the classification of diradicals into two types depending on whether their NBMO's can be confined to disjoint sets of atoms provides a useful basis for understanding the electronic properties. It has been proposed that by consideration of the effect of electron repulsion, the triplet is relatively stabilized at the SCF level when two singly occupied (SO) NBMO's of the triplet state are nondisjoint compared with each other.[8]

First, let us consider the SOMO's of $^3HTA^{2+}$ in Figure 4a, which clearly shows that their patterns are of a nondisjoint type. From this point of view, it can be understood that, as shown in

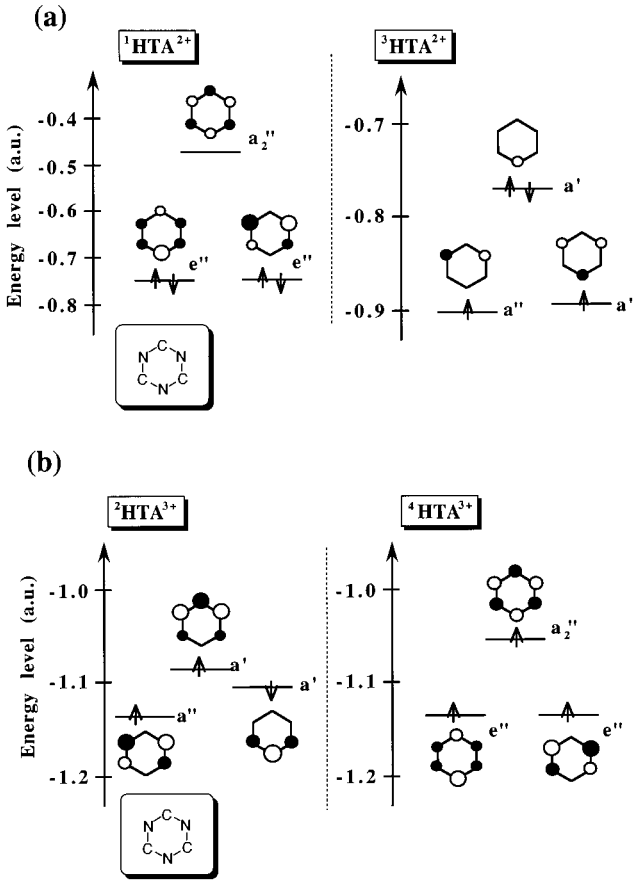

Figure 4. Energy levels and patterns of the frontier MO's of (a) dicationic states, $^1HTA^{2+}$ and $^3HTA^{2+}$ and (b) tricationic states, $^2HTA^{3+}$ and $^4HTA^{3+}$. Note that $^3HTA^{2+}$ and $^2HTA^{3+}$ are nonplanar.

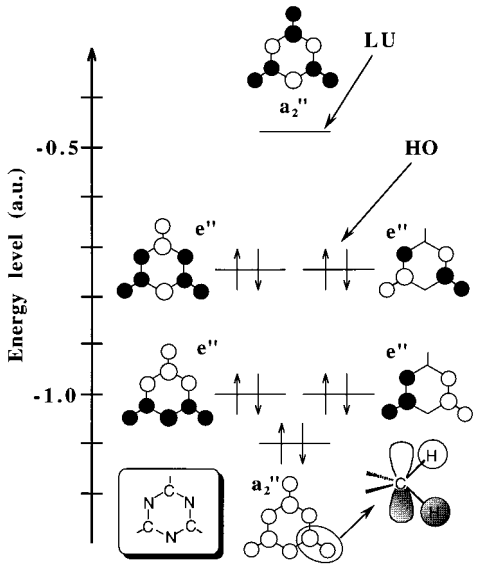

Figure 5. Energy levels and orbital patterns of the π-type MO's of $^1HTA^{2+}$.

Table 3, the energetic state of $^3HTA^{2+}$ lies well below that of $^1HTA^{2+}$ at the UHF level.

On the other hand, the SOMO patterns of $^3TA^{2+}$ correspond to those of e′(a_1) and e′(b_2), as discussed in the previous section. Those SOMO's are degenerate, and their patterns seem to be of a nondisjoint type. Hence, as shown in Table 3, it is plausible that the energetic state of $^3TA^{2+}$ again lies well below that of $^1TA^{2+}$ at the UHF level, similar to HTA.

TABLE 4: Total Atomic and π-Spin Densities[a] of TA Species

	$^3TA^{2+}$		$^2TA^{3+}$ (II)		$^4TA^{3+}$	
	total	π	total	π	total	π
C1	−0.567	−0.384	−0.270	−0.139	−0.616	−0.397
N1	1.198	0.387	1.171	0.167	1.564	0.402
C2	−0.567	−0.384	−0.111	−0.089	−0.616	−0.397
N2	1.198	0.387	−0.893	−0.010	1.564	0.402
C3	−0.567	−0.384	−0.111	−0.089	−0.616	−0.397
N3	1.198	0.387	1.171	0.167	1.564	0.402

[a] The π-spin density is defined as the summation of the 2pπ and 3pπ spin densities.

TABLE 5: Total Atomic and π-Spin Densities[a] of HTA Species

	$^3HTA^{2+}$		$^2HTA^{3+}$		$^4HTA^{3+}$	
	total	π^b	total	pseudo π	total	π
C1	−0.229		−0.221	−0.057	−0.227	−0.057
N1	1.139		1.118	0.917	1.132	0.925
C2	−0.103		−0.001	−0.000	−0.227	−0.057
N2	0.003		−1.104	−0.911	1.132	0.925
C3	−0.103		−0.001	−0.000	−0.227	−0.057
N3	1.139		1.118	0.917	1.132	0.925

[a] The π-spin density is defined as the summation of the 2pπ and 3pπ spin densities. [b] Cannot be determined due to nonplanar triazine ring.

6. Magnetic Interaction Due to the Spin Correlation

6.1. Spin Polarization and Through-Bond Interaction. The calculated total atomic spin densities together with the π-spin densities on the carbon and nitrogen atoms of the TA and HTA series are listed in Tables 4 and 5, respectively. The atomic spin densities on the hydrogen atoms that are smaller by more than 1 order of magnitude are not listed here. There is a partial spin polarization on the ring, where large positive spin densities are mainly localized on the nitrogen atoms and negative ones on the carbon atoms. In the high-spin states (triplets and quartets), polarization of the spin densities are clearly seen, which ought to contribute to the ferromagnetic interaction between the spins on the nitrogen atoms. That is, the through-bond ferromagnetic interaction would exist in triplets and quartets of TA and HTA.

6.2. Estimation of Through-Space Interaction. In open-shell TA species, rather large spin densities on the nitrogen atoms are of a σ-type from the σ-type SOMO's such as e′(a_1) and e′(b_2) shown in Figure 2 while more than one-half of the value of these spin densities on the carbon atoms are of π character (Table 4). It should be mentioned that since SOMO's of these species are σ-type, these π-spin densities are considered to be induced by the σ-electrons of the SOMO's. The values of the π-spin densities on the nitrogen atoms are almost the same as those on the carbon atoms. Hence, these open-shell cationic TA species are considered as a $\sigma-\pi$ mixed-spin system being, in a sense, similar to that of a polycarbene.[33] Note that although the total spin densities in $^4TA^{3+}$ become larger compared with $^3TA^{2+}$, the distribution of the π-spin densities is similar in these two species. In other words, the σ-spin densities mainly increase in changing from $^3TA^{2+}$ to $^4TA^{3+}$.

Due to the facility of overlapping, the through-space interaction between the pσ-type spins is larger than that between the pπ-type ones. Thus, the N1−N3 pσ-type spin interaction in the e′(a_1) SOMO of $^3TA^{2+}$ would bring about a certain instability to the system from its through-space magnetic interaction. However, as mentioned above, the stabilization of $^3TA^{2+}$ is in turn expected from the through-bond magnetic interaction of pπ-type spins due to the usual spin polarization. Thus, $^3TA^{2+}$ is considered to intrinsically have these two kinds of magnetic interactions and, in total, is finally stabilized by the pπ-type through-bond interaction including the carbon atoms. On the other hand, it is considered that $^4TA^{3+}$ has a more serious instability from the through-space interaction among the nitrogen atoms than $^3TA^{2+}$ while there would not be such a large difference in the stability from the through-bond interaction between $^3TA^{2+}$ and $^4TA^{3+}$.

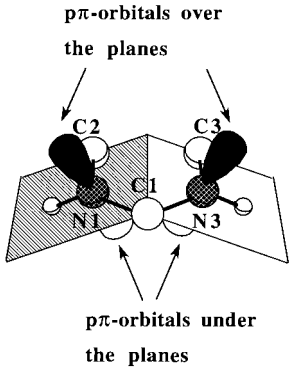

Figure 6. Schematic representation of the configuration of pπ orbitals on nitrogen atoms of $^3HTA^{2+}$.

TABLE 6: Calculated Energies at the MP2 and MP3/6-31G Levels

	MP2 level		MP3 level	
	energy/ hartree	E_{rel}[a]/ kcal·mol^{-1}	energy/ hartree	E_{rel}[a]/ kcal·mol^{-1}
$^1TA^{2+}$(I)	−278.5703		−278.5666	
$^3TA^{2+}$	−278.5784	−5.08	−278.5926	−16.32 (more stable)
$^2TA^{3+}$(II)	−277.7037		−277.7402	
$^4TA^{3+}$	−277.6629	+25.60	−277.7069	+20.90 (less stable)
$^1HTA^{2+}$	−282.2893		−282.3007	
$^3HTA^{2+}$	−282.2457	+27.36	−282.2994	+0.82 (less stable)
$^2HTA^{3+}$	−281.5530		−281.6127	
$^4HTA^{3+}$	−281.5495	+2.20	−281.6098	+1.82 (less stable)

[a] Stabilization energy of the high-spin state compared with the corresponding lower-spin state.

In open-shell HTA species, the gross orbital population analysis suggests that these spin densities on the nitrogen atoms are of a pseudo-π-type except those in $^3HTA^{2+}$. Therefore, it is expected that there is a small contribution of the through-space interaction among the nitrogen atoms to the instability of $^2HTA^{3+}$ and $^4HTA^{3+}$ compared with TA.

On the other hand, the case of $^3HTA^{2+}$ is very unique. $^3HTA^{2+}$ has two nitrogen atoms (N1 and N3) on which large spin densities are localized. The two amino groups containing the N1 and N3 atoms adopt locally "planar" conformations, as illustrated in Figure 6. According to the gross orbital population, the spin-bearing atomic orbitals on these nitrogen atoms are mainly of a π-type with respect to each plane. However, it is considered that the interaction between the pπ orbitals on these nitrogen atoms are not so strong compared with the pure pπ−pπ interaction, and hence, the contribution of the through-space magnetic interaction in $^3HTA^{2+}$ could become larger than that in the usual π-conjugated planar system.

7. Spin Multiplicity of Each Ground State

The calculated energies for the different spin states of the cationic states of TA and HTA at the MP2 and MP3/6-31G* levels are listed in Table 6. It is seen that the third-order perturbation gives larger stabilization (or destabilization) energies of the higher-spin states.

The singlet−triplet energy splitting ΔE_{S-T} of TA^{2+} by UHF/6-31G* is 47.88 kcal/mol (cf. Table 3), which is reduced to 16.32 kcal/mol after the MP3 correction, predicting that the ground state of TA^{2+} is a triplet, probably due to the nondisjoint type of SOMO's. There can be two reasons for this reduction: (i) a pσ−pσ through-space magnetic interaction mentioned above causes a certain amount of instability in $^3TA^{2+}$ and (ii) the excited singlet state of $^1TA^{2+}$ becomes relatively stable due to the two kinds of locally optimized structures (I and II), as listed in Table 1, or in other words, a meta-stable excited state $^1TA^{2+}$ (II) could make some contribution to stabilization. From Table 6, the ground state of TA^{3+} is suggested to be a doublet, with the doublet−quartet energy splitting ΔE_{D-Q} being 20.83 kcal/mol at the MP3/6-31G* level while 4.20 kcal/mol at the UHF/6-31G* level (cf. Table 3). This difference could be due to inclusion of the through-space magnetic interaction in the MP3 correction as discussed above.

On the other hand, the values of E_{rel} for HTA^{2+} and HTA^{3+} at the MP3 level, suggest that there are no remarkable differences (less than 2 kcal/mol) in the energies between the high- and low-spin states. This signifies that the high- and low-spin states will be almost degenerate in these species. As discussed in the previous section, there should be a large contribution to the stability in $^3HTA^{2+}$ by means of the effect of the electron repulsion and through-bond interaction. However, inclusion of the MP3 level stabilizes the pseudoaromatic system of $^1HTA^{2+}$ due to the configuration interaction of double excitation to the lowest unoccupied (LU) MO, making $^1HTA^{2+}$ and $^3HTA^{2+}$ almost degenerate.

Extending the discussion to dications $^3TA^{2+}$ and $^3HTA^{2+}$, $^4HTA^{3+}$ should be stabilized by the electron repulsion effect, since the SOMO patterns are of a nondisjoint type (Figure 4). However, the structure of $^2HTA^{3+}$ is optimized under a lower symmetry constraint (C_s) in order to include the static effect of the Jahn−Teller distortion as described above, and hence, there might be a slight stability occurring from the slight distortion of the triazine ring in $^2HTA^{3+}$. Because of these complex factors, $^2HTA^{3+}$ and $^4HTA^{3+}$ would be, indeed, degenerate at the UHF level. In any case, it is considered that there would not be large differences between the configuration interactions in $^2HTA^{3+}$ and $^4HTA^{3+}$ based on the MP3 correction and, consequently, that these two states are predicted to be almost degenerate at the MP3 level.

8. Concluding Remarks

We have investigated the electronic structures of the neutral and cationic states of TA and HTA by the MP3/6-31G* calculations. The values of the energy splitting between high- and low-spin states vary rather largely by the MP3 correction, and hence, it is suggested that including the electron correlation is essential for prediction of the ground states of cationic TA and HTA species, probably concerning the magnetic stability. According to the present results, the spin densities are largely localized on the nitrogen atoms. Clearer spin polarization are seen in the high-spin states (i.e., $^3TA^{2+}$, $^4TA^{3+}$, $^3HTA^{2+}$, and $^4HTA^{3+}$), which is expected to contribute to the ferromagnetic interaction between spins on the nitrogen atoms in the through-bond manner. In TA, the multiplicity of the ground state of TA^{2+} is predicted to be triplet while that of TA^{3+} a doublet. Moreover, analysis of the electronic structures indicates that their spin systems contain both σ- and π-type spins.

On the other hand, in HTA, the double-excitation configuration interaction would largely stabilize $^1HTA^{2+}$ having the pseudoaromatic electronic system and, therefore, $^1HTA^{2+}$ and $^3HTA^{2+}$ can become almost degenerate at the MP3 level. $^2HTA^{3+}$ and $^4HTA^{3+}$ are also predicted to be almost degenerate, probably due to inclusion of the Jahn−Teller effect. These results strongly suggest that TA^{2+} turns out to be a good candidate for the high-spin organic molecule and, moreover, that HTA^{2+} and HTA^{3+} would become candidates of σ-radical spin systems with bistability on the spin multiplicity.

Acknowledgment. This work is a part of the project of the Institute for Fundamental Chemistry, supported by Japan Society for the Promotion of Science−Research for the Future Program (JSPS-RFTF96P00206). Numerical calculations were carried out in part at the Supercomputer Laboratory of the Institute for Chemical Research of Kyoto University.

References and Notes

(1) Heisenberg, W. *Z. Phys.* **1928**, *49*, 636.
(2) Kinoshita, N.; Turek, P.; Tamura, M.; Nozawa, K.; Shiomi, D.; Nakazawa, Y.; Ishikawa, M.; Takahashi, M.; Awaga, K.; Inabe, T.; Maruyama, Y. *Chem. Lett.* **1991**, 1225.
(3) Mataga, N. *Theor. Chim. Acta* **1968**, *10*, 372.
(4) Breslow, R. *Pure Appl. Chem.* **1982**, *54*, 927.
(5) Awaga, K.; Sugano, T.; Kinoshita, N. *Chem. Phys. Lett.* **1987**, *141*, 540.
(6) Yamaguchi, K.; Toyoda, Y.; Fueno, T. *Synth. Met.* **1987**, *19*, 81.
(7) Fukutome, H.; Takahashi, A.; Ozaki, M. *Chem. Phys. Lett.* **1987**, *133*, 34.
(8) Borden, W. T.; Davidson, E. R. *J. Am. Chem. Soc.* **1977**, *99*, 4587.
(9) Iwamura, H. *Pure Appl. Chem.* **1986**, *58*, 187.
(10) Yoshizawa, K.; Chano, A.; Ito, A.; Tanaka, K.; Yamabe, T.; Fujita, H.; Yamauchi, J.; Shiro, M. *J. Am. Chem. Soc.* **1992**, *114*, 5994.
(11) Yoshizawa, K.; Hatanaka, M.; Matsuzaki, Y.; Tanaka, K.; Yamabe, T. *J. Chem. Phys.* **1994**, *100*, 4453.
(12) Torrance, J. B.; Oostra, S.; Nazzal, A. *Synth. Met.* **1987**, *19*, 709.
(13) Ovchinnikov, A. A.; Spector, V. N. *Synth. Met.* **1988**, *27*, B615.
(14) Ota, M.; Otani, S.; Kobayashi, K.; Igarashi, M. *Mol. Cryst. Liq. Cryst.* **1989**, *176*, 99.
(15) Kawabata, K.; Mizutani, M.; Fukuda, M.; Mizogami, S. *Synth. Met.* **1989**, *33*, 399.
(16) Mizogami, S.; Mizutani, M.; Fukuda, M.; Kawabata, K. *Synth. Met.* **1991**, *41*−*43*, 3271.
(17) Tanaka, K.; Kobashi, M.; Sanekata, H.; Takata, A.; Yamabe, T.; Mizogami, S.; Kawabata, K.; Yamauchi, J. *J. Appl. Phys.* **1992**, *71*, 836.
(18) Murata, K.; Ushijima, H.; Ueda, H.; Kawaguchi, K. *J. Chem. Soc., Chem. Commun.* **1991**, 1265.
(19) Prasad, B. L. V.; Radhakrishnan, T. P. *J. Phys. Chem. A* **1997**, *101*, 2973.
(20) Osamura, Y.; Unno, M.; Hashimoto, K. *J. Am. Chem. Soc.* **1987**, *109*, 1370.
(21) Kato, H.; Hirao, K.; Yamashita, K. *J. Mol. Struct. (THEOCHEM)* **1982**, *88*, 265.
(22) Habibollahzadeh, D.; Grodzicki, M.; Seminario, J. M.; Politzer, P. *J. Phys. Chem.* **1991**, *95*, 7699.
(23) Poppinger, D.; Radom, L.; Vincent, M. A. *Chem. Phys.* **1977**, *23*, 437.
(24) Borden, W. T.; Davidson, E. R.; Feller, D. *Tetrahedron* **1982**, *38*, 737.
(25) Raghavachari, K.; Haddon, R. C.; Miller, T. A.; Bondybey, V. E. *J. Chem. Phys.* **1983**, *79*, 1387.
(26) Rossi, A. R.; Avouris, P. *J. Chem. Phys.* **1983**, *79*, 3413.
(27) Saebø, S.; Radom, L.; Schaefer, H. F., III *J. Chem. Phys.* **1983**, *78*, 845.
(28) Krogh-Jespersen, K.; Roth, H. D. *J. Am. Chem. Soc.* **1992**, *114*, 8388.
(29) Frisch, M. J.; Trucks, G. W.; Schlegel, H. B.; Gill, P. M. W.; Johnson, B. G.; Robb, M. A.; Cheeseman, J. R.; Keith, T.; Petersson, G. A.; Montgomery, J. A.; Raghavachari, K.; Al-Laham, M. A.; Zakrzewski, V. G.; Ortiz, J. V.; Foresman, J. B.; Cioslowski, J.; Stefanov, B. B.; Nanayakkara, A.; Challacombe, M.; Peng, C. Y.; Ayala, P. Y.; Chen, W.; Wong, M. W.; Andres, J. L.; Replogle, E. S.; Gomperts, R.; Martin, R. L.; Fox, D. J.; Binkley, J. S.; Defrees, D. J.; Baker, J.; Stewart, J. P.; Head-Gordon, M.; Gonzalez, C.; Pople, J. A. *Gaussian 94*, Revision C.3; Gaussian, Inc.: Pittsburgh, PA, 1995.
(30) Szabo, A.; Ostlund, N. S. *Modern Quantum Chemistry*; Macmillan: New York, 1982; Chapter 3.
(31) Marquardt, R.; Sander, W.; Kraka, E. *Angew. Chem., Int. Ed. Engl.* **1996**, *35*, 746.
(32) Wierschke, S. G.; Nash, J. J.; Squires, R. R. *J. Am. Chem. Soc.* **1993**, *115*, 11958.
(33) Tanaka, K.; Shichiri, T.; Yamabe, T. *J. Mol. Struct.* (*THEOCHEM)* **1989**, *188*, 313.